In Vivo ^{31}P-NMR Diffusion Spectroscopy of ATP and Phosphocreatine in Rat Skeletal Muscle

Robin A. de Graaf, Arnaud van Kranenburg, and Klaas Nicolay
Department of Experimental In Vivo NMR, Image Sciences Institute, University Medical Center, Utrecht, the Netherlands

ABSTRACT The aim of this study was to measure the diffusion of ATP and phosphocreatine (PCr) in intact rat skeletal muscle, using ^{31}P-NMR. The acquisition of the diffusion-sensitized spectra was optimized in terms of the signal-to-noise ratio for ATP by using a frequency-selective stimulated echo sequence in combination with adiabatic radio-frequency pulses and surface coil signal excitation and reception. Diffusion restriction was studied by measuring the apparent diffusion coefficients of ATP and PCr as a function of the diffusion time. Orientation effects were eliminated by determining the trace of the diffusion tensor. The data were fitted to a cylindrical restriction model to estimate the unbounded diffusion coefficient and the radial dimensions of the restricting compartment. The unbounded diffusion coefficients of ATP and PCr were ~90% of their in vitro values at 37°C. The diameters of the cylindrical restriction compartment were ~16 and ~22 μm for ATP and PCr, respectively. The diameters of rat skeletal muscle fibers are known to range from 60 to 80 μm. The modelling therefore suggests that the in vivo restriction of ATP and PCr diffusion is not imposed by the sarcolemma but by other, intracellular structures with an overall cylindrical orientation.

INTRODUCTION

NMR spectroscopy allows the noninvasive study of metabolism in living systems. Phosphorus-31 has been a prominent nucleus for in vivo NMR studies since the first reports of its application to biological samples (Moon and Richards, 1973; Hoult et al., 1974). In vivo ^{31}P-NMR is primarily used for bioenergetic studies because it allows the measurement of molecules like phosphocreatine (PCr), adenosine triphosphate (ATP), and inorganic phosphate (P_i), as well as intracellular pH (for a review see Radda, 1992). Knowledge of the intracellular diffusive transport of the high-energy phosphates PCr and ATP is crucial for the quantitative description of mammalian bioenergetics. NMR diffusion measurements of PCr and ATP provide an exceptional means of probing the barriers to diffusion in the cytoplasmic space, in terms of both their dimensions and their orientation.

A major goal of this study was to design a NMR pulse scheme that would allow the measurement of ATP diffusion with sufficient sensitivity. To that end, a frequency-selective stimulated echo sequence was developed that refocuses J-modulation of the ATP resonances. The sequence is based on the use of adiabatic radiofrequency pulses, in combination with a surface coil for signal excitation and reception. The apparent diffusion coefficients of PCr and ATP were determined as a function of the diffusion time and in three orthogonal directions, to account for the effects of diffusion restriction and diffusion anisotropy, respectively. The unrestricted diffusion coefficients of PCr and ATP and the dimensions of the restricting compartment were estimated by modeling the experimental data under the assumption of cylindrical symmetry. This choice was based on the fact that the cellular units of skeletal muscle, the muscle fibers, and the major constituent of the sarcoplasm, the myofibrils, have an elongated, cylindrical shape (Salmons, 1995).

This is the first study to report on the diffusion characteristics of ATP in intact skeletal muscle in situ.

THEORY

Below we will first explain the novel elements of the NMR pulse scheme that made possible the quantitation of ATP diffusion in intact muscle. Thereafter, the basic theory of NMR diffusion measurements in homogeneous and heterogeneous systems that formed the basis of the data evaluation is summarized.

Adiabatic stimulated echo sequence

The measurement of the diffusion coefficient of ATP (and, to a lesser extent, that of PCr) by ^{31}P-NMR spectroscopy poses a number of challenges. First, NMR of low gyromagnetic nuclei like ^{31}P is an insensitive technique that makes the measurement of the ATP diffusion coefficient in vivo a challenge in terms of sensitivity. Second, diffusion measurements by pulsed field gradient NMR spectroscopy require that the nuclear magnetization spend a certain time in the transverse plane. The transverse magnetization is therefore inevitably decreased by T_2 relaxation, particularly for ATP, which has a T_2 of 20–30 ms. Third, the phosphate nuclei within the ATP molecule are all scalar coupled, which leads to signal loss in echo sequences when left uncompensated. These three factors complicate the mea-

Received for publication 22 July 1999 and in final form 12 December 1999.

Address reprint requests to Dr. Klaas Nicolay, Department of Experimental In Vivo NMR, Image Sciences Institute, University Medical Center Utrecht, Bolognalaan 50, 3584 CJ Utrecht, the Netherlands. Tel.: +30-2535569; Fax: +30-2535561; E-mail: nicolay@invivonmr.uu.nl.

Dr. de Graaf's present address is Magnetic Resonance Center, Yale University School of Medicine, P.O. Box 208043, New Haven, CT 06520-8043.

0006-3495/00/04/1657/08 $2.00

surement of ATP and explain why most in vivo ^{31}P-NMR diffusion measurements of ATP suffer from a relatively poor signal-to-noise ratio (Moonen et al., 1990; Yoshizaki et al., 1990; Van Gelderen et al., 1994; Hubley and Moerland, 1995; Hubley et al., 1995). Often only PCr diffusion data are presented (Moonen et al., 1990; Van Gelderen et al., 1994; Kinsey et al., 1999). PCr has a reasonably long T_2 (~170 ms), is present at relatively high concentrations compared to ATP, and has a singlet resonance.

Surface coils are among the most sensitive NMR antennae and are therefore frequently used for in vivo studies. When the surface coil is not only used for signal reception, but also for transmission of conventional RF pulses, signal losses arise. This is because the nutation angle of such RF pulses is directly proportional to the generated RF field, which is inherently inhomogeneous for surface coils. To eliminate these RF-related signal losses, we decided to employ adiabatic excitation pulses (Garwood and Ke, 1991; Garwood and Ugurbil, 1992; De Graaf and Nicolay, 1997). Adiabatic pulses are amplitude- and frequency-modulated RF pulses, capable of generating a uniform nutation angle throughout the sensitive volume of the coil, independent of the RF amplitude.

A stimulated echo sequence is the most appropriate NMR pulse sequence for the study of translational diffusion of compounds with short T_2 relaxation times (Moonen et al., 1990; Van Gelderen et al., 1994). Fig. 1 *A* shows a conventional stimulated echo sequence, executed with three adiabatic 90° BIR-4 RF pulses. Pulsed magnetic field gradients, executed during the two TE/2 periods, sensitize the NMR signal to translational diffusion. The influences of T_1 and T_2 relaxation, diffusion, scalar coupling, and frequency offsets can be evaluated using the product operator formalism (Sørensen et al., 1983). For a scalar coupled, two-spin system the density matrix of nucleus I at the top of the echo is given by

$$\sigma_I(\mathrm{TE}+\mathrm{TM}) = \frac{I_y}{2}(1-e^{-\mathrm{TM}/T_1})e^{-\mathrm{TE}/T_2}e^{-b\cdot\mathrm{ADC}}\cos(\pi J\mathrm{TE}) \quad (1)$$

in which TE is the echo time; TM is the mixing time; T_1 and T_2 are the longitudinal and transverse relaxation times, respectively; b is the diffusion-weighting factor (see below); ADC is the apparent diffusion coefficient; and J is the spin-spin coupling constant.

The stimulated echo represents 50% of the maximally achievable signal, because only 50% of the transverse magnetization is along the longitudinal axis during TM. It can also be seen from Eq. 1 that T_1 relaxation affects the magnetization during TM, while T_2 relaxation is only operative during TE. Therefore, by choosing a relatively short TE and a long TM period, the diffusion labeling time can be long, without introducing large signal losses due to T_2 relaxation. The last term in Eq. 1 arises from J-evolution during TE for scalar coupled spins. At practical echo times that allow sufficient time to incorporate the pulsed magnetic field gradients, the cosine term in Eq. 1 accounts for a large part of the signal losses associated with the pulse sequence in Fig. 1 *A*. The signal intensity for scalar coupled spin systems like ATP would therefore significantly increase when J-evolution during TE is refocused. The sequence shown in Fig. 1 *B* generates a selective stimulated echo and indeed is capable of refocusing the J-evolution of α- and γ-ATP. The SSAP pulse (De Graaf et al., 1995) is the adiabatic analog of a jump-return pulse that achieves semi-selective excitation. In this study, the β-ATP resonance was not excited, while the other resonances were excited according to a frequency-dependent sinusoidal excitation profile. The product operator evaluation of the pulse sequence in Fig. 1 *B* gives the following expression for the magnetization of a scalar coupled, two-spin system at the top of the echo:

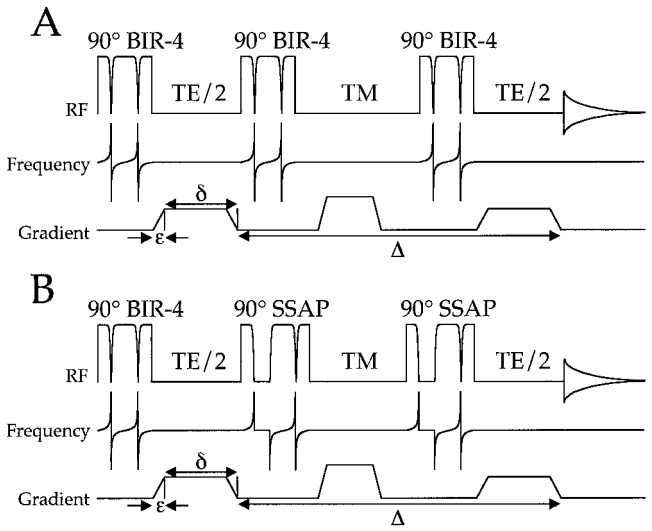

FIGURE 1 NMR pulse sequences for the generation of (*A*) a nonselective stimulated echo and (*B*) a selective stimulated echo. (*A*) The nonselective sequence employs adiabatic 90° BIR-4 pulses, for which the RF amplitude and frequency modulations are shown. Diffusion sensitization is achieved by magnetic field gradients in the two TE/2 periods. The individual magnetic field gradients are characterized by ϵ and δ, the gradient ramping time and pulselength, respectively. The magnetic field gradients are separated by a delay Δ. The third magnetic field gradient during TM is a TM-crusher gradient used to dephase transverse magnetization. (*B*) The selective sequence is executed with two adiabatic, frequency-selective SSAP pulses. These RF pulses have no effect on the β-ATP resonance, while the α- and γ-ATP resonances are simultaneously rotated over a frequency-dependent nutation angle (which is ideally 90°). As a consequence, J-evolution during TE will be refocused. Further details are given in the text.

$$\sigma_I(\mathrm{TE}+\mathrm{TM}) = \frac{I_y}{2}(1-e^{-\mathrm{TM}/T_1})e^{-\mathrm{TE}/T_2}e^{-b\cdot\mathrm{ADC}}\sin^2(2\pi\omega\tau) \quad (2)$$

The cosine term for J-evolution has vanished and has been replaced by a sine-squared term describing the excitation

profile of the two SSAP pulses. By adjusting the intrapulse delay within the SSAP pulse, the frequency of maximum excitation can be adjusted. Therefore, the sine-squared term in Eq. 2 can be made unity for one ATP resonance (α or γ), while the other resonances experience slight signal losses. By using appropriate values for J-coupling constants and the SSAP excitation profile, it can be estimated that the selective stimulated echo sequence generates almost three times more signal than the conventional stimulated echo sequence.

Isotropic diffusion

Stejskal and Tanner (1965) have shown that NMR experiments can be sensitized to diffusion by the use of pulsed magnetic field gradients (Fig. 1). The general expression for the signal attenuation ($S(\mathbf{G})/S(0)$) due to unrestricted diffusion is given by

$$\ln\left(\frac{S(\mathbf{G})}{S(0)}\right) = -\gamma^2 \int_0^t \left(\int_0^{t'} \mathbf{G}(t'')\mathrm{d}t'' \right) \cdot \mathbf{D} \cdot \left(\int_0^{t'} \mathbf{G}(t'')\mathrm{d}t'' \right) \mathrm{d}t \tag{3}$$

$S(\mathbf{G})$ and $S(0)$ are the signal intensities in the presence and absence of diffusion sensitizing gradients, $\mathbf{G}$ is a gradient vector, and $\mathbf{D}$ is a rank two tensor given by

$$\mathbf{D} = \begin{pmatrix} D_{xx} & D_{xy} & D_{xz} \\ D_{yx} & D_{yy} & D_{yz} \\ D_{zx} & D_{zy} & D_{zz} \end{pmatrix} \tag{4}$$

For isotropic solutions, the diffusion coefficient is independent of the direction along which it is measured, i.e., all elements of the diffusion tensor $\mathbf{D}$ are equal. For rectangular magnetic field gradients, Eq. 3 then becomes

$$\ln\left(\frac{S(G)}{S(0)}\right) = -\gamma^2 G^2 \delta^2 \left(\Delta - \frac{\delta}{3}\right) D = -bD \tag{5}$$

in which $\mathbf{G}$ is the gradient strength, δ is the duration of the gradient pulse, Δ is the gradient separation, and the b value is a measure of the strength of the diffusion weighting.

The mean square displacement λ of the molecule investigated is given by the Einstein equation:

$$\lambda^2 = 2Dt_{\mathrm{dif}} \tag{6}$$

in which t_{dif} is the diffusion time that equals ($\Delta - \delta/3$) for rectangular magnetic field gradients. Equation 6 is very useful because the displacement is the actual physical property that is measured.

Anisotropic diffusion

In vivo the presence of physical restricting barriers (e.g., cell membranes) makes the effective diffusion coefficient dependent on the shape, the size, and the permeability of the restricting barriers as well as on the diffusion time and the direction of diffusion sensitization. The measured diffusion coefficient is commonly referred to as the apparent diffusion coefficient (ADC). The restriction effects necessitate complete knowledge of the diffusion tensor to adequately describe the diffusion process. When the restriction elements have cylindrical symmetry on a macroscopic scale, the diffusion tensor $\mathbf{D}'$ in the tissue frame of reference simplifies to

$$\mathbf{D}' = \begin{pmatrix} D_\perp & 0 & 0 \\ 0 & D_\perp & 0 \\ 0 & 0 & D_\parallel \end{pmatrix} \tag{7}$$

where $D_\perp$ and $D_\parallel$ are the diffusion coefficients as measured perpendicular and parallel to the cylinder axis, respectively. The off-diagonal elements in the diffusion tensor $\mathbf{D}'$ of Eq. 7 are zero in the tissue frame of reference. However, the diffusion coefficients are measured in the gradient frame of reference in which diffusion is described by the diffusion tensor $\mathbf{D}$ (Eq. 4). Because the gradient frame generally does not coincide with the tissue frame of reference, all elements of $\mathbf{D}$ are nonzero. We have adopted the approach to the orientational dependence of the diffusion coefficients that has been suggested by Van Gelderen et al. (1994) and others (Basser et al., 1994; LeBihan, 1995). The approach uses the trace of the diffusion tensor because this property is invariant to rotation:

$$\begin{aligned} \mathrm{Tr}(\mathbf{D}) &= (D_{xx} + D_{yy} + D_{zz}) = (2D_\perp + D_\parallel) \\ &= \mathrm{Tr}(\mathbf{D}') = 3D_{\mathrm{Tr}} \end{aligned} \tag{8}$$

D_{Tr}, which will be referred to here as the trace diffusion coefficient, is the average of the diffusion coefficients measured separately in the x, y, and z directions. The use of the trace of the diffusion tensor implies that the results are not affected by the orientation of the sample in the magnet or the distribution of fiber orientations in the muscle complex.

The signal attenuation in a diffusion experiment (with two gradient pulses of amplitude G, duration δ, and separation Δ) for the case of diffusion sensitization parallel and perpendicular to the main cylinder axis in the case of cylindrical boundaries is given by (Neuman, 1974; Van Gelderen et al., 1994)

$$\ln\left(\frac{S}{S_0}\right) = -\gamma^2 G^2 D_{\mathrm{f}} \delta^2 \left(\Delta - \frac{\delta}{3}\right) \tag{9}$$

and

$$\ln\left(\frac{S}{S_0}\right) = -2\gamma^2 G^2 \times \sum_{m=1}^{\infty} \frac{2C_m\delta - 2 + 2e^{-C_m\delta} + 2e^{-C_m\Delta} - e^{-C_m(\Delta-\delta)} - e^{-C_m\Delta+\delta)}}{C_m^2 \alpha_m^2 (R^2\alpha_m^2 - 1)} \tag{10}$$

respectively, in which $C_m = D_f\alpha_m^2$. D_f is the unbounded diffusion coefficient, R is the radius of the cylinder, and α_m are the roots of the equation

$$J_1'(\alpha_m R) = 0 \quad (11)$$

J_1' is the derivative of a Bessel function of the first kind, order one.

The modeling of the experimental data that was based on the above expressions assumes a finite diameter and an infinite length of the cylindrical compartment, i.e., restriction effects are assumed to play a role only in the radial and not in the axial direction.

MATERIALS AND METHODS

The experiments were performed using a Varian (Palo Alto, CA) spectrometer interfaced to a 4.7-T Oxford magnet equipped with a high-performance gradient insert (220 mT/m in 300 μs). In vivo experiments were conducted on adult male Wistar rats (300–375 g, $n = 6$) that were mechanically ventilated with N_2O/O_2 (7:3) and 0.8% halothane. Body temperature was kept at 37 ± 1°C by means of a water-heated pad. The RF pulse was transmitted and the NMR signal received with a two-turn surface coil (Ø 25 mm) tuned to the phosphorus frequency (80.984 MHz). The surface coil was positioned on the skeletal muscle of the left hindleg, which includes the gastrocnemius, plantaris, and soleus muscles. Except for the inherent localization provided by the surface coil, no spatial localization was used to maximize sensitivity and to avoid potential cross-terms between diffusion gradients and volume selection gradients.

Diffusion-weighted spectra were acquired with the pulse sequence shown in Fig. 1 *B*, using a repetition time TR = 5.0 s, echo time TE = 20 ms, number of acquisitions NA = 128, acquisition time = 51 ms over a spectral width of 2500 Hz. The frequency offset of the selective SSAP pulses (corresponding to the nulling frequency) was set on the β-ATP resonance, while the intrapulse delay was adjusted to give maximum excitation of the γ-ATP resonance. The duration of the BIR-4 and SSAP pulses was 2.0 ms, with modulation functions as previously described (Garwood and Ke, 1991).

Diffusion sensitization was accomplished using magnetic field gradients (Fig. 1) in which the ramp time ϵ was set at 300 μs, while the gradient pulselength δ was 9.3 ms. To measure the apparent diffusion coefficients, six different amplitudes of the diffusion gradients were used, resulting in b values ranging from 100 s·mm^{-2} to ~4000 s·mm^{-2} at maximum, depending on the TM time. The acquisition of three separate data sets, in which the diffusion gradient was applied in the x, y, or z direction, allowed the calculation of the apparent D_{xx}, D_{yy}, and D_{zz}, using Eq. 4. The average of these represents the trace diffusion coefficient (Eq. 8). Restriction effects were assessed by determining the trace diffusion coefficient as a function of the diffusion time t_{dif}. The diffusion time was changed by increasing the TM delay. TM was chosen to be 37.5, 75, 150, 300, 500, 800, and 1200 ms.

In vitro ^{31}P-NMR diffusion experiments were performed using the above stimulated echo sequence, on two different spherical samples containing 1) 40 mM PCr, 25 mM ATP, 15 mM P_i, and 30 mM $MgCl_2$ (pH 7.2); and 2) 25 mM ADP and 30 mM $MgCl_2$ (pH 7.2). ^{31}P-NMR was performed as above, except that TM was 50, 100, 200, 400, and 800 ms. ^{1}H-NMR experiments of Cr and water diffusion were carried out on a sample containing 40 mM Cr (pH 7.2), using a one-turn surface coil (Ø 20 mm) tuned to a proton frequency of 200.1 MHz, and TR = 5.0 s, NA = 32, and TE = 10 ms. For the ^{1}H studies, the SSAP pulses were used for water suppression. In vitro experiments were performed at 20°C and at 37°C. The sample temperature was maintained with the aid of a warm water circulation system. The in vitro data were averaged from four independent experiments.

The NMR spectra were analyzed with the time-domain fitting routine VARPRO (Van der Veen et al., 1988). The resonances were fitted with Lorentzian lineshapes. After fitting the first spectrum of a series without constraints, all following spectra were fitted with fixed linewidths, phases, and chemical shift positions. α- and γ-ATP were both fitted as a doublet (^2J = 18.5–22.0 Hz).

The signal attenuation curves were fitted to a single exponential function to yield the apparent diffusion coefficient. The data points that related the trace diffusion coefficient to the diffusion time were fitted with a gradient-expansion algorithm written within IDL (Interactive Data Language; Research Systems, Boulder, CO) to obtain the unbounded diffusion coefficient D_f and the radius of the cylindrical boundary R, according to Eqs. 9 and 10, following the procedure used by Van Gelderen et al. (1994).

RESULTS

Fig. 2 shows ^{31}P-NMR spectra from rat skeletal muscle, as measured as a function of the echo time TE. The spectra were acquired with the nonselective and the selective stim-

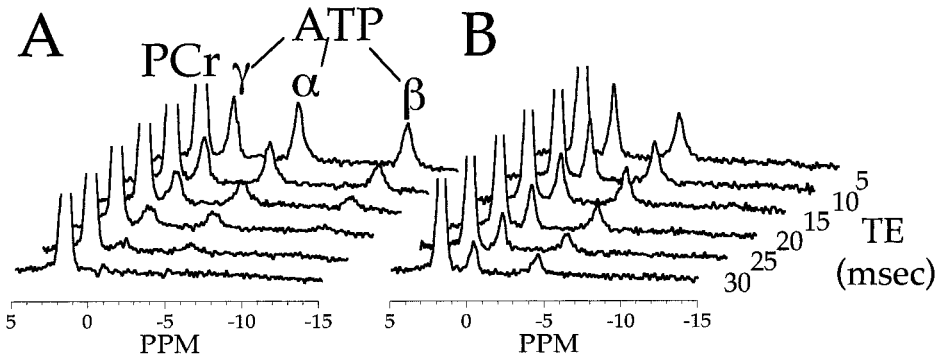

FIGURE 2 ^{31}P-NMR spectra of rat skeletal muscle measured as a function of the echo time TE for (*A*) the nonselective and (*B*) the selective NMR pulse sequences as shown in Fig. 1, *A* and *B*, respectively. The β-ATP resonance is not visible in *B*, because of the frequency-selective excitation profile of the SSAP pulses. However, because J-evolution is refocused in *B*, the α- and γ-ATP signal intensities at longer echo times (TE > 20 ms) are substantially higher than those obtained with the nonselective NMR pulse sequence (*A*). The PCr peak is cut off to allow a better visualization of the ATP peaks. Note that the relative peak intensities in *B* are affected by the excitation profile of the SSAP pulses. This explains the difference in intensity of the α- and γ-ATP peaks. TM was 75 ms.

ulated echo sequences as depicted in Fig. 1, *A* and *B*, respectively. Fig. 2 shows that the NMR signal decreased with prolongation of the echo time, as expected. However, in the case of the selective sequence the α- and γ-ATP signals persisted at longer echo times (compare Fig. 2, *A* and *B*) because their attenuation was no longer affected by *J*-modulation effects. In subsequent in vivo diffusion measurements a TE of 20 ms was used. Fig. 2 *B* demonstrates that appreciable ATP signal persists at this echo time when the new pulse scheme is used.

The diffusion coefficients of inorganic phosphate (P_i), phosphocreatine (PCr), and ATP were measured under in vitro conditions. These measurements in a homogeneous medium serve as a reference point for the in vivo studies. As expected, the diffusion coefficients were independent of TM because diffusion is unrestricted in this case (data not shown). In addition, the diffusion coefficients of creatine (Cr) and water were measured using ^{1}H-NMR. The in vitro diffusion coefficients measured at 20°C and 37°C are summarized in Table 1. At 37°C, the diffusion coefficients of all molecules tested were ~50% higher than at 20°C. These data are in good agreement with values in the literature (Moonen et al., 1990; Nicolay et al., 1995; Hubley et al., 1996; Kinsey et al., 1999).

Two representative sets of diffusion-weighted ^{31}P-NMR spectra from intact skeletal muscle are shown in Fig. 3. Six spectra were acquired with different gradient strengths, and the magnetic field gradient direction was approximately parallel (Fig. 3 *A*) or perpendicular (Fig. 3 *B*) to the muscle fiber direction. Signal attenuation is more prominent in Fig. 3 *A* than in Fig. 3 *B*. This is a manifestation of diffusion anisotropy. The effect is not only evident for the PCr resonance but, because of the good signal-to-noise ratio, also clearly visible for the α- and γ-ATP resonances.

Measurements such as those in Fig. 3 were carried out for three orthogonal gradient directions and as a function of diffusion time. Fig. 4 *A* gives a typical example of the integrated signal intensities for PCr and α- and γ-ATP as a function of the diffusion-weighting factor *b* (Eq. 5) for the three different directions. The trace diffusion coefficients, as calculated from data exemplified in Fig. 4 *A*, are shown in Fig. 4 *B* as a function of the TM period. The diffusion restriction is evident from the decrease in the trace diffusion coefficient with increasing TM times. The solid lines in Fig. 4 *B* represent the best fit according to Eqs. 9 and 10. Fig. 4 *C* shows the mean square displacement as a function of TM. The dotted line represents the mean square displacement when assuming unrestricted diffusion, and its deviation from the experimental curve is another manifestation of the restrictions imposed on PCr and ATP diffusion in vivo. The unbounded diffusion coefficients D_f and the radius *R* were obtained by modeling the data for a cylindrical diffusion compartment (Table 2). D_f of PCr and ATP as determined in vivo were ~86% and ~95% of the in vitro diffusion coefficients at 37°C (Table 1), respectively. The limiting radii for ATP and PCr were estimated to amount to ~8 and ~11 μm, respectively. The data analysis for the γ- and α-phosphates in ATP yielded essentially identical results.

TABLE 1 Diffusion coefficients *D* of metabolites *in vitro*, as measured at 20°C and 37°C*

	D (10^{-9} m^2 · s^{-1})	
	T, 20°C	*T*, 37°C
P_i	0.59 ± 0.09	0.95 ± 0.07
PCr	0.48 ± 0.05	0.74 ± 0.04
ATP†	0.35 ± 0.05	0.53 ± 0.06
Cr‡	0.63 ± 0.05	0.91 ± 0.03
ADP†	0.33 ± 0.04	0.52 ± 0.05
Water‡	1.93 ± 0.02	3.00 ± 0.02

**In vitro* samples contained 1) 40 mM PCr, 25 mM ATP, and 30 mM $MgCl_2$; 2) 25 mM ADP and 30 mM $MgCl_2$; or 3) 40 mM Cr (pH 7.2).
†The ADC of ATP is the average of the values for the γ- and α-phosphates. The ADC of ADP was determined from the signal of the terminal β-phosphate.
‡Measured with ^{1}H-NMR spectroscopy.

DISCUSSION

The in vivo measurement of the diffusion coefficient of metabolites by NMR poses a challenge because of the low inherent sensitivity of NMR and is further complicated by signal losses associated with T_1 and T_2 relaxation and by *J*-evolution in the case of scalar-coupled spins. A diffusion-sensitized NMR pulse sequence was presented that minimizes most of the above signal losses and allows the detailed characterization of the diffusion properties of PCr and ATP under in vivo conditions.

The diffusion NMR experiments were done as a function of the direction and the duration of diffusion sensitization. The data are indicative of diffusion restriction and anisotropy effects that appear to be similar for PCr and ATP. The relationship between the trace of the diffusion tensor and the diffusion time was assumed to be governed by cylindrical geometry, inspired by the macroscopic and microscopic structural features of skeletal muscle (Salmons, 1995). The modeling, which yielded satisfactory fits of the experimental data, produced two significant results. First, the unbounded diffusion coefficients D_f of PCr and ATP in vivo approached in vitro values. Similar values have been reported for PCr by Kinsey et al. (1999) in excised goldfish red and white muscle and by Van Gelderen et al. (1994) in rabbit hindlimb. Second, the diameter of the cylindrical restriction elements was estimated to be 16 and 22 μm for ATP and PCr, respectively. Similar numbers were found for PCr in rabbit muscle (Van Gelderen et al., 1994). Our data show that the diffusion characteristics of ATP and PCr are comparable in vivo. This is a plausible result because the two metabolites probe the same intracellular compartment in skeletal muscle. There are no transport systems that

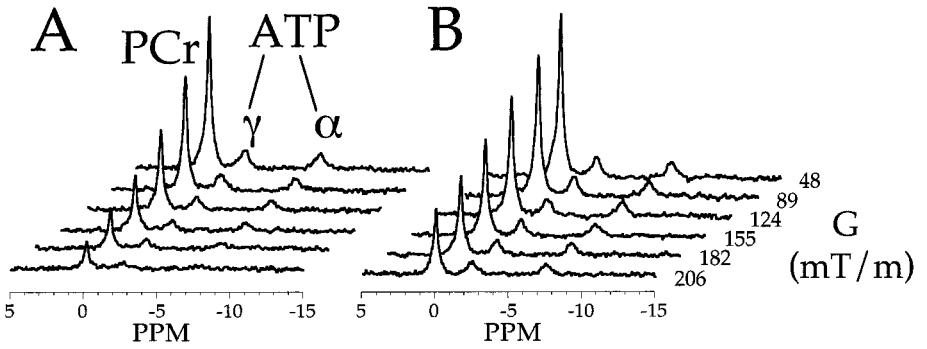

FIGURE 3 Typical diffusion-weighted ^{31}P-NMR spectra from rat hindleg skeletal muscle in vivo acquired at TM = 75 ms. Diffusion sensitization was performed (*A*) in the *z* direction (which was approximately parallel to the muscle fibers) and (*B*) in the *x* direction of the gradient frame of reference (which was approximately perpendicular to the muscle fibers). The diffusion weighting increases from back to front. The diffusion anisotropy is clearly visible for both the PCr and ATP resonances.

mediate the transfer of PCr across membranes. Therefore, this charged molecule is entrapped in the cytoplasmic compartment of the myocyte. In contrast, ATP has access to other parts of the muscle cell, including the mitochondrial matrix space. However, because the mitochondrial density is relatively low in the muscle complex sampled, the ATP diffusion data also primarily report on the cytoplasmic compartment. Further study is required to establish whether the slightly smaller diameter of the restricting element for ATP as compared to PCr is significant.

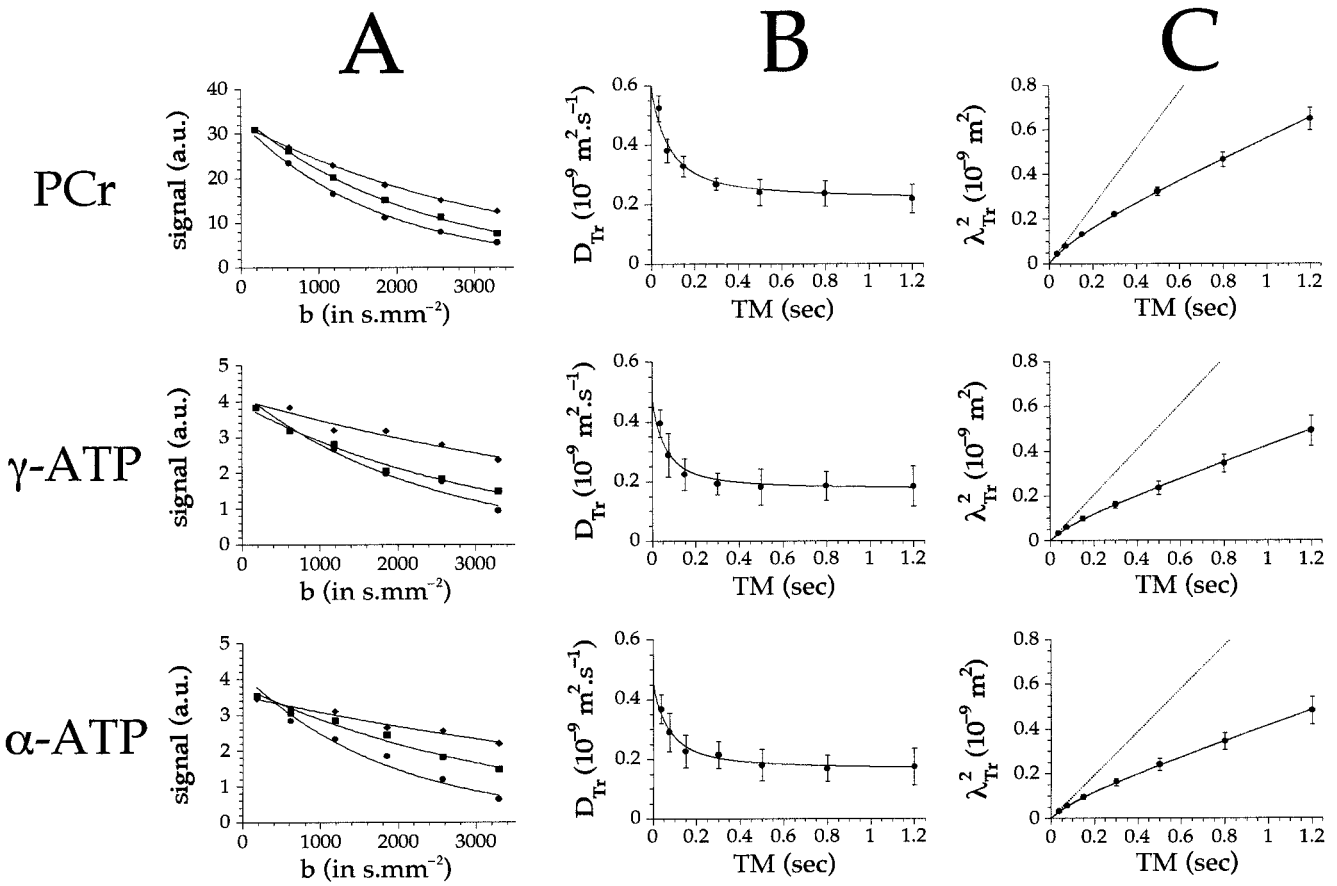

FIGURE 4 In vivo diffusion of PCr and ATP in rat skeletal muscle. (*A*) Integrated signal intensities for PCr and α- and γ-ATP as a function of the *b* value (TM = 75 ms). The curves were fitted with a monoexponential function to estimate the apparent diffusion coefficient. The diffusion anisotropy is evident from the curves for the different gradient directions *x* (♦), *y* (■), and *z* (●). (*B*) Trace diffusion coefficient D_{Tr} for PCr and α- and γ-ATP as a function of TM (which is proportional to the diffusion time). Each experimental point is the average of six independent measurements ± standard deviation. The solid line represents the best fit to the experimental data according to Eqs. 9 and 10. (*C*) Trace mean square displacement λ^2_{Tr} for PCr, and α- and γ-ATP as a function of TM. λ^2_{Tr} was calculated from the (time-dependent) trace diffusion coefficient D_{Tr} as shown in *B*, according to Eq. 6. The solid lines are the best fit to the experimental data. The dotted lines indicate the mean square displacement when the unrestricted diffusion coefficient $D_{Tr}(0)$, as obtained from the modeling in *B*, is used in Eq. 6. The difference between the dotted and solid lines is again indicative of diffusion restriction.

TABLE 2 Unbounded diffusion coefficients D_f for PCr and α- and γ-ATP and radius of cylindrical boundary

	D_f (10^{-9} m$^2 \cdot$ s^{-1})	R (10^{-6} m)
PCr	0.64 ± 0.07	10.7 ± 0.9
γ-ATP	0.51 ± 0.08	8.2 ± 1.0
α-ATP	0.49 ± 0.09	8.8 ± 1.1

Van Gelderen et al. (1994) have proposed that PCr diffusion in the radial dimension of the myocyte is limited by the sarcolemma. The diameters of muscle fibers in rat hindlimb are known to range from ~60 μm for fast-type IIA fibers in gastrocnemius muscle (Schluter and Fitts, 1994; de Ruiter et al., 1995) and for slow-twitch fibers in soleus muscle (McDonald and Fitts, 1995) to ~80 μm for slow-type I fibers in soleus muscle and fast-type IIB fibers in gastrocnemius muscle (Schluter and Fitts, 1994). Therefore, we favor the interpretation that the diffusional anisotropy in rat muscle results from intracellular barriers well within the boundaries of the sarcolemma. Kinsey et al. (1999) have recently studied PCr diffusion anisotropy in isolated goldfish muscle. Their data also provided convincing evidence that the radial restriction does not involve the cell membrane. In addition, the time scale over which changes in diffusion occurred indicated that interactions of PCr with the thick and thin filament lattice of actin and myosin were not involved. Kinsey et al. (1999) hypothesize, rather, that the sarcoplasmic reticulum and mitochondria are the principal intracellular structures that restrict diffusional transport of PCr in an orientation-dependent manner. Both have dimensions on the micron length scale and have a structural organization that is compatible with the observed anisotropy. Further experimentation is warranted to substantiate this interesting hypothesis.

The NMR signal that forms the basis of our diffusion assessment originated from a mixture of fiber types. It cannot be excluded that metabolite diffusion differs among fiber types. However, Moerland and co-workers have reported that the effective diffusion coefficient of PCr is very similar in different fiber types of fish muscle (Hubley et al., 1997; Kinsey et al., 1999), suggesting that the cytoplasmic compartment poses similar barriers to diffusion in these tissues, despite their functional differences. It should be stressed that the current analysis procedure is insensitive to the distribution of fiber orientations in the sensitive volume of the NMR receiver coil. The results possibly are affected by the presence of nonmuscle tissue in the sensitive volume of the coil. This is considered a minor issue because the ATP and PCr content of this tissue is low.

The measured in vivo ADC values of PCr and ATP provide useful information concerning the diffusive intracellular transport that connects the free-energy delivering sites (e.g., mitochondria) and the free-energy utilizing sites in the muscle cell (e.g., myofibrils). ATP can essentially be transported by two different mechanisms: 1) direct diffusion (Jacobus, 1985) and 2) facilitated diffusion (Meyer et al., 1984) in which PCr diffuses to sites of ATP utilization and is used to rephosphorylate ADP via creatine kinase activity. Diffusion of Cr to the ATP-delivering sites and its phosphorylation by local creatine kinase species close the Cr/PCr cycle (Wallimann et al., 1992; Nicolay et al., 1998). The net flux J of metabolites by direct diffusion is proportional to $D_f * (dC/dr)$, i.e., the product of the free diffusion coefficient and the concentration gradient. Realistic in vivo concentrations for metabolites in rat skeletal muscle are [PCr] = 20 mM, [ATP] = 5 mM, [Cr] = 8 mM, and [ADP] = 0.02 mM. Our data show that the unbounded in vivo diffusion coefficients of PCr and ATP are ~90% of their in vitro values. Therefore, the unbounded in vivo diffusion coefficients of Cr and ADP are estimated to be 0.82 and 0.47×10^{-9} m$^2 \cdot$s^{-1}, respectively. Assuming equal concentration gradients, it can be shown that $J_{PCr} \approx 5J_{ATP}$ and $J_{Cr} \gg J_{ADP}$. This would imply that direct diffusion may suffice for ATP transport to the myofibrils (forward flux), but that the CK-mediated facilitated diffusion mechanism is highly favorable for the return of ADP equivalents to the mitochondria. When the facilitated diffusion model of Meyer et al. (1984) is considered, it nevertheless can be shown that >99.8% of the forward flux is also carried by PCr/Cr because of the near-equilibrium CK system. Therefore, direct diffusion of ADP and ATP will only play a significant role in the absence of cytoplasmic CK. Direct adenine nucleotide diffusion will suffice for short diffusion lengths (<2 μm) but may be expected to limit metabolic capacity for longer diffusion distances. It should be noted that the above calculation made use of the estimated unbounded diffusion coefficients, while diffusive transport over length scales of tens of microns will strongly reduce the effective diffusion coefficients. This situation will make the role of indirect diffusive transport of ATP/ADP via the PCr/Cr couple even more prominent. Evidence in support of the proposal that direct ATP/ADP diffusion may limit the capacity of energy metabolism is provided by findings in transgenic mice lacking the cytoplasmic M-type CK isoenzyme. Skeletal muscle in these animals lacks burst activity and shows increased mitochondrial density, especially in the myofibrillar compartment (Van Deursen et al., 1993). This adaptation causes a reduction of the mean diffusion path lengths of the adenine nucleotides between mitochondria and myofibrils.

The present findings may contribute to the debate on the constitution of the intracellular milieu. The in vivo unbounded diffusion coefficients of both ATP and PCr approach in vitro values. This suggests that the viscosity of the aqueous cytoplasm is not much lower than that of water. Wheatly and co-workers (Agutter et al., 1995; Wheatley, 1998) have recently postulated that diffusion has only a minor role in metabolic activity and is "assisted" in many aspects of cell physiology. NMR diffusion spectroscopy measures molecular displacement and is not able to discrim-

inate diffusion per se (in the sense of random Brownian motion) from "assisted" diffusion. Further experimentation is required to assess the physical mechanisms that underly the apparent diffusivity of ATP and PCr that was found in this study.

We gratefully acknowledge Gerard van Vliet for his expert technical assistance and Rick Dijkhuizen and Erwin Blezer for their help with the animal experiments.

REFERENCES

Agutter, P. S., P. C. Mallone, and D. N. Wheatley. 1995. Intracellular transport mechanisms: a critique of diffusion theory. *J. Theor. Biol.* 176:261–272.

Basser, P. J., J. Mattiello, and D. LeBihan. 1994. MR diffusion tensor spectroscopy and imaging. *Biophys. J.* 66:259–267.

De Graaf, R. A., Y. Luo, M. Terpstra, H. Merkle, and M. Garwood. 1995. A new localization method using an adiabatic pulse, BIR-4. *J. Magn. Reson. B.* 106:245–252.

De Graaf, R. A., and K. Nicolay. 1997. Adiabatic RF pulses: applications to in vivo NMR. *Concepts Magn. Reson.* 9:247–268.

de Ruiter, C. J., A. de Haan, and A. J. Sargeant. 1995. Physiological characteristics of two extreme muscle compartments in gastrocnemius medialis of the anaesthetized rat. *Acta Physiol. Scand.* 153:313–324.

Garwood, M., and Y. Ke. 1991. Symmetric pulses to induce arbitrary flip angles with compensation for RF inhomogeneity and resonance offsets. *J. Magn. Reson.* 94:511–525.

Garwood, M., and K. Ugurbil. 1992. B_1 insensitive adiabatic RF pulses. *In* NMR Basic Principles and Progress, Vol. 27. P. Diehl, E. Fluck, H. Gunther, R. Kosfeld, and J. Seelig, editors. Springer-Verlag, Berlin. 109–147.

Hoult, D. I., S. J. W. Busby, D. G. Gadian, G. K. Radda, R. E. Richards, and P. J. Seeley. 1974. Observations of tissue metabolites using ^{31}P nuclear magnetic resonance. *Nature Lond.* 252:285–287.

Hubley, M. J., B. R. Locke, and T. S. Moerland. 1996. The effects of temperature, pH and magnesium on the diffusion coefficient of ATP in solutions of physiological ionic strength. *Biochim. Biophys. Acta.* 1291: 115–121.

Hubley, M. J., B. R. Locke, and T. S. Moerland. 1997. Reaction-diffusion analysis of the effects of temperature on high-energy phosphate dynamics in goldfish skeletal muscle. *J. Exp. Biol.* 200:975–988.

Hubley, M. J., and T. S. Moerland. 1995. Application of homonuclear decoupling to measures of diffusion in biological ^{31}P spin echo spectra. *NMR Biomed.* 8:113–117.

Hubley, M. J., R. C. Rosanske, and T. S. Moerland. 1995. Diffusion coefficients of ATP and creatine phosphate in isolated muscle: pulsed gradient ^{31}P-NMR of small biological samples. *NMR Biomed.* 8:72–78.

Jacobus, W. E. 1985. Theoretical support for the heart phosphocreatine energy transport shuttle based on the intracellular diffusion limited mobility of ADP. *Biochem. Biophys. Res. Commun.* 133:1035–1041.

Kinsey, S. T., B. R. Locke, B. Penke, and T. S. Moerland. 1999. Diffusional anisotropy is induced by subcellular barriers in skeletal muscle. *NMR Biomed.* 12:1–7.

LeBihan, D. 1995. Diffusion and Perfusion Magnetic Resonance Imaging. Raven Press, New York.

Mattiello, J., P. J. Basser, D., and LeBihan. 1994. Analytical expressions for the b matrix in NMR diffusion imaging and spectroscopy. *J. Magn. Reson. A.* 108:131–141.

McDonald, K. S., and R. H. Fitts. 1995. Effect of hindlimb unloading on rat soleus fiber force, stiffness, and calcium sensitivity. *J. Appl. Physiol.* 79:1796–1802.

Meyer, R. A., H. L. Sweeney, and M. J. Kushmerick. 1984. A simple analysis of the "phosphocreatine shuttle." *Am. J. Physiol.* 15: C365–C377.

Moon, R. B., and J. H. Richards. 1973. Determination of intracellular pH by ^{31}P magnetic resonance. *J. Biol. Chem.* 248:7276–7278.

Moonen, C. T. W., P. C. M. van Zijl, D. LeBihan, and D. DesPres. 1990. In vivo NMR diffusion spectroscopy: ^{31}P application to phosphorus metabolites in muscle. *Magn. Reson. Med.* 13:467–477.

Neuman, C. H. 1974. Spin echo of spins diffusing in a bounded medium. *J. Chem. Phys.* 60:4508–4511.

Nicolay, K., A. van der Toorn, and R. M. Dijkhuizen. 1995. In vivo diffusion spectroscopy. An overview. *NMR Biomed.* 8:365–374.

Nicolay, K., F. A. Van Dorsten, T. Reese, M. J. Kruiskamp, J. F. Gellerich, and C. J. A. Van Echteld. 1998. NMR-based in situ measurements of creatine kinase flux. The lessons from bioengineered mice. *Mol. Cell. Biochem.* 184:195–208.

Price, W. S. 1997. Pulsed-field gradient nuclear magnetic resonance as a tool for studying translational diffusion. Part 1. Basic theory. *Concepts Magn. Reson.* 9:299–336.

Radda, G. K. 1992. Control, bio-energetics and adaptation in health and disease from nuclear magnetic resonance. *FASEB J.* 6:3032–3038.

Salmons, S. 1995. Skeletal muscle. *In* Gray's Anatomy, 38th Ed. Churchill Livingstone, London. 738.

Schluter, J. W., and R. H. Fitts. 1994. Shortening velocity and ATPase activity in rat skeletal muscle fibers: effects of endurance exercise training. *Am. J. Physiol.* 266:C1699–C1713.

Sørensen, O. W., G. W. Eich, M. H. Levitt, G. Bodenhausen, and R. R. Ernst. 1983. Product operator formalism for the description of NMR pulse experiments. *Prog. NMR Spectrosc.* 16:163–192.

Stejskal, E. O., and J. E. Tanner. 1965. Spin diffusion measurements: spin echoes in the presence of a time-dependent field gradient, *J. Chem. Phys.* 42:288–292.

Van der Veen, J. W. C., R. de Beer, P. R. Luyten, and D. van Ormondt. 1988. Accurate quantification of in vivo ^{31}P-NMR signals using the variable projection method and prior knowledge. *Magn. Reson. Med.* 6:92–98.

Van Deursen, J., A. Heerschap, F. Oerlemans, W. Ruitenbeek, P. Jap, H. ter Laak, and B. Wieringa. 1993. Skeletal muscles of mice deficient in muscle creatine kinase lack burst activity. *Cell.* 74:621–631.

Van Gelderen, P., D. DesPres, P. C. M. van Zijl, and C. T. W. Moonen. 1994. Evaluation of restricted diffusion in cylinders. Phosphocreatine in rabbit leg muscle. *J. Magn. Reson. B.* 103:255–260.

Wallimann, T., M. Wyss, D. Brdiczka, K. Nicolay, and H. M. Eppenberger. 1992. Intracellular compartmentation, structure and function of creatine kinase isoenzymes in tissues with high and fluctuating energy demands: the "phosphocreatine circuit" for cellular energy homeostasis. *Biochem. J.* 281:21–40.

Wheatley, D. N. 1998. Diffusion theory, the cell and the synapse. *BioSystems.* 45:151–163.

Yoshizaki, K., H. Watari, and G. K. Radda. 1990. Role of phosphocreatine in energy transport in skeletal muscle of bullfrog studied by ^{31}P-NMR. *Biochim. Biophys. Acta.* 1051:144–150.